THE JOURNAL OF PHYSICAL CHEMISTRY C
A JOURNAL OF THE AMERICAN CHEMICAL SOCIETY

pubs.acs.org/JPCC

Article

Element-Specific Magnetization Dynamics in Co−Pt Alloys Induced by Strong Optical Excitation

Published as part of The Journal of Physical Chemistry virtual special issue "D. D. Sarma Festschrift".

Igor Vaskivskyi,* Rameez Saeed Malik, Leandro Salemi, Diego Turenne, Ronny Knut, Jeffrey Brock, Robert Stefanuik, Johan Söderström, Karel Carva, Eric E. Fullerton, Peter M. Oppeneer, Olof Karis, and Hermann A. Dürr*

Cite This: *J. Phys. Chem. C* 2021, 125, 11714−11721

Read Online

ACCESS | Metrics & More | Article Recommendations

ABSTRACT: Ever since its first observation, the microscopic origin of ultrafast magnetization dynamics has been actively debated. Even more questions arise when considering composite materials featuring a combination of intrinsic and proximity-induced magnetic moments. Currently, it is unknown whether the specific ultrafast dynamics of different sublattices in the popular ferromagnets consisting of 3d (Co, Fe) and 4d, 5d (Pd, Pt) transition metals are playing a crucial role in various effects, including all-optical magnetization switching. Here we investigate the element-specific dynamics of Co−Pt alloys on femtosecond and picosecond time scales using magneto-optical spectroscopy in the extended ultraviolet (EUV) region. Our results reveal that despite the proximity-induced nature of the magnetization of Pt atoms, the two sublattices in the alloy can have different responses to the optical excitation featuring distinct demagnetization rates. Additionally we show that it is important to consider the modification of magnetic anisotropy in opto-magnetic experiments as the vast majority of them are sensitive only to a single projection of the magnetic moment on the predefined axis, which may lead to experimental artifacts.

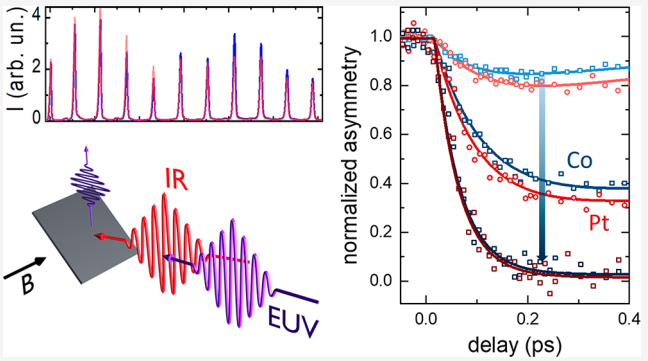

INTRODUCTION

In addition to fundamental interest, the field of ultrafast magnetism[1−3] is greatly driven by the technological demand for new types of digital storage media and integrated opto-magnetic devices. Currently available magnetic storage devices have difficulty matching the ever-increasing amount of data generated in the world. Simple scaling of the current technology has already reached limits, and thus fundamentally new approaches must be developed to create smaller and faster devices that hopefully consume less energy. In the former case, the superparamagnetic limit is the fundamental limitation, which may be overcome by using magnetically harder materials with strong magnetic anisotropy. While this may improve data sustainability and the reliability of small data bits, it becomes difficult to record the magnetic data patterns. Several approaches, including heat- or light-assisted magnetic recording or even all-optical magnetization reversal,[4−6] are being pursued. While the latter is probably of most interest due to the possibility to reach ultimate recording speeds, it is also the least understood.

The single-pulse all-optical magnetization reversal in composite ferrimagnets[5,7−10] is attributed to the presence of two antiferromagnetically coupled lattices with significantly different dynamics (e.g., a fast transition metal and slower rare-earth element). This effect can be observed by using linearly polarized light, with each subsequent laser pulse toggling the magnetic orientation. The reverted state, in this case, is reached via a transient ferromagnetic configuration on a time scale of a few picoseconds.

The specifics of the microscopic processes responsible for the helicity-dependent all-optical magnetization switching in ferromagnets[11,12] are still under debate. In most cases, a long train of laser pulses is required to trigger the reversal. However, there have been several works suggesting that the process can

Received: March 15, 2021
Revised: May 11, 2021
Published: May 24, 2021

be optimized to work with a few[13] or even a single light pulse. A specific combination of short and long optical pulse with precisely tuned delay allowed to achieve switching after just four laser pulses,[14] and in some conditions, magnetization reversal was triggered by a single laser pulse.[15] However, in the latter case, the process was still slow, with the sample reaching the new magnetic state several microseconds after the pulse, suggesting that heat dissipation and domain processes might play an important role. Single-pulse all-optical switching can also be achieved by combining a ferromagnetic layer with a ferrimagnetic layer that is either exchange-coupled or separated by a metallic spacer. In this case, the magnetization reversal in the ferrimagnet can also trigger the transition on the ferromagnetic layer.[16,17] However, to the best of our knowledge, there is no experimental proof of single-pulse all-optical magnetization reversal triggered inside the ferromagnet on the picosecond time scale without additional ferrimagnetic structures.

The fact that the light-induced switching of magnetization in ferromagnets has only been observed in systems with more than one magnetic sublattice suggests that, similar to the case of ferrimagnets, the details of the element-specific magnetization dynamics may be the key enabling factor for this phenomenon. The most used ferromagnets that exhibit all-optical magnetization reversal are combinations of 3d (Co, Fe) and 4d, 5d (Pd, Pt) transition metals in alloys or multilayers[12,18] where the nonmagnetic 4d/5d element gain a net magnetization due to proximity effects. While it is often anticipated that proximity-induced magnetization should follow the same dynamics as the "driving" magnetic moment, there are still some controversies. Combined resonant X-ray magnetic circular dichroism (XMCD) and magneto-optical Kerr spectroscopy (MOKE) measurements with near-IR light have revealed a significant difference in the dynamics of the intrinsic Fe and induced Pt magnetic moments in FePt films[19] on a picosecond time scale. However, in another experiment, resonant transversal MOKE (TMOKE) spectroscopy with EUV photons on a similar material showed no difference in the demagnetization of the two sublattices.[20] While the latter experiment has the advantage of measuring the complete data set in a single experiment with a broadband laser source, the partial overlap of the absorption edges of Fe and Pt in the probed spectral range potentially compromises the element specificity of the measurement. The former study, on the other hand, had its complication from comparing two essentially different experiments, so it might be prone to other artifacts.

In this work, we study element-specific spin dynamics in Co−Pt alloys by employing time-resolved resonant transversal magneto-optical Kerr spectroscopy (tr-TMOKE) in the EUV spectral range. Co/Pt-based materials were among the first ferromagnets, in which all-optical magnetization switching was observed.[11] Granular Co−Pt media has already been implemented in real-world storage devices. The system features a combination of intrinsic Co magnetic moments and proximity-induced magnetism on the Pt sublattice. The incorporation of Pt atoms with their large spin−orbit coupling enhances the overall magnetization dynamics relative to pure Co,[21] as has been shown in all-optical studies. All-optical experiments in the near-IR, however, cannot resolve whether the magnetization of the two sublattices follows the same dynamics.

We choose EUV TMOKE as an experimental technique because, depending on the core level energies, it can allow for the resolution of element-specific dynamics by tuning to core−valence resonances with no intrinsic timing jitter between different spectral components, provided the core-level energies are sufficiently separated. An additional advantage of the resonant TMOKE is the strength of the signal at the chosen scattering angle of 90°, which is about 10 times stronger[22] compared to XMCD in the EUV range.[23]

METHODS

Sample Growth and Characterization. We prepared the Co−Pt samples by dc magnetron sputtering using a cosputtering technique. Having determined the deposition rate of Co and Pt by using X-ray reflectivity measurements, the sample stoichiometry was controlled by varying the power supplied to each target during the sputtering process. Here we present the results for 30 nm thick Co70Pt30 (at. %) samples. X-ray diffraction measurements demonstrated that samples grown on Si substrates with a 300 nm thick SiOx coating using a 3 nm thick Ta seed layer (sample A) exhibited a (111) out-of-plane texture, whereas samples deposited on a 5 nm thick epitaxial Cr (211) layer grown on MgO(110) (sample B) have an hcp texture with the *c*-axis oriented in the plane of the substrate. The sample thickness, alloy composition, and growth temperatures were optimized to produce easy-plane samples with a coercivity of ∼50 mT for transversal MOKE experiments. Unless otherwise stated, the sample grown on Si/SiOx (sample A) is used throughout the paper. Given that the Co−Pt layer is significantly larger than the penetration depth of both the optical and HHG beams, reflection from the bottom surface of the films need not be considered.

Experimental Setup. Element-specific magnetization dynamics were measured via the resonant time-resolved transversal magneto-optical Kerr effect (tr-TMOKE) in the range 40−72 eV. The output of the amplified Ti:sapphire 35 fs pulsed laser source with the central wavelength at 800 nm (Coherent Legend Elite Duo) was split into two parts: around 90% of the laser power was directed into the probe leg, where the beam was spatially filtered and tightly focused into the gas cell, filled with ∼1 bar of He gas. Via the high harmonic generation process, a part of the strong optical beam is converted into the EUV photons with the broad spectrum consisting of odd harmonics of the driving laser light.[24,25] After the HHG gas cell, the fundamental 800 nm light is filtered out by a thin-film Al filter, and the broadband EUV beam is focused onto the sample by using a set of off-axis parabolic mirrors to a spot size of ∼50 μm FWHM.

The pump beam, after attenuation, is directed through the optical delay line and is focused on the same area of the sample with a slightly larger focal spot of ∼150 μm FWHM to overfill the probed region. The pump and the probe beams are propagating nearly collinearly before hitting the sample to ensure good time resolution. The sample is rotated at ∼45° to the incoming beams. Both the probe and the pump beams are p-polarized. By working near the Brewster angle, we maximize the signal[22] and minimize the background caused by the residue of the s-polarized probe photons, which do not contribute to magnetic contrast.

The light reflected from the sample surface is directed into a Rowland-type EUV spectrometer, where it is first filtered by a thin-film Al filter (to block the pump photons) and is dispersed by a curved diffraction grating on an MCP detector with a phosphor screen. The image of the screen is then recorded with an in-air optical camera.

https://doi.org/10.1021/acs.jpcc.1c02311
J. Phys. Chem. C 2021, 125, 11714−11721

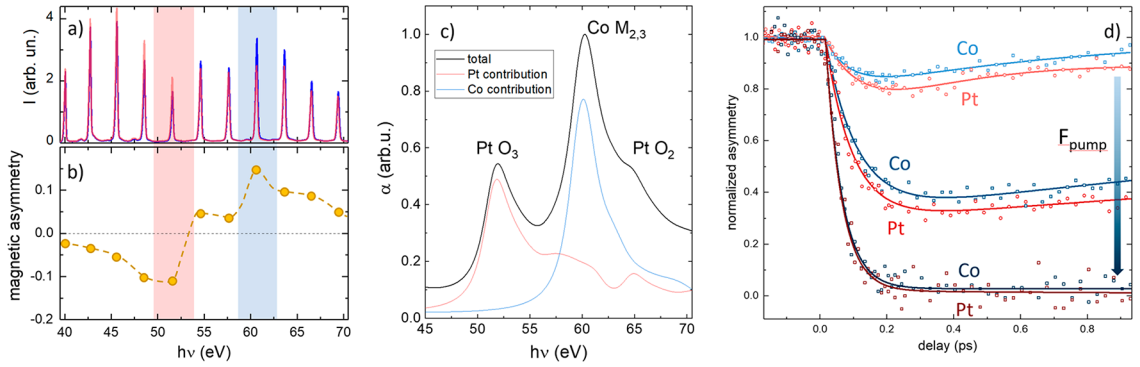

Figure 1. Static reflectivity of Co−Pt alloy measured with the p-polarized EUV light and two opposite directions of the external magnetic field (a). Static magnetic asymmetry of the sample measured in TMOKE geometry. Solid circles are experimental data, and the dashed line is a guide for the eye (b). The error bars in (a) and (b) are not visible due to low noise level. Ab initio computed absorption spectrum of $Co_{0.5}Pt_{0.5}$ with the positions of the Co and Pt core levels indicated. Red and blue curves represent the contribution of Pt and Co transitions, respectively (c). Time evolution of magnetic asymmetry measured close to Co 3p−3d (shades of blue) and Pt 5p−5d (shades of red) resonances for different pump fluences with 1.5 eV pump (d).

The sample chamber has a dipole electromagnet, which allows for the application of a magnetic field up to 0.2 T perpendicular to the plane of incidence of the laser beam.

The spectrum of the reflected beam was recorded as a function of pump and probe time delay for two opposite directions of the external magnetic field. An example of a typical spectrum is shown in Figure 1a. The magnetic asymmetry for each time delay was then calculated as $A = (I_+ - I_-)/(I_+ - I_-)$, where I_+ and I_- are the intensities of the reflected probe beam for the two opposite orientations of the magnetic field (Figure 1a,b).

The time- and element-resolved hysteresis loops were measured in the same geometry, with the magnitude of the external magnetic field cycled between the collection of each delay point.

For all time traces and hysteresis loops, the spectral data were integrated across the bandwidth of the corresponding harmonic (~200 meV). Because the spectral response in the whole range of 40−72 eV is measured simultaneously, it allows us to compare the time dynamics at different energies with ultimate precision with no need to correct for any kind of time jitters. More details about the experimental setup can be found elsewhere.[26]

DFT Calculations. To provide insight into the element-dependent demagnetization process of the Co−Pt alloy, we performed density functional theory (DFT) calculations of the electronic structure of CoPt. We used the relativistic full-potential linearized augmented plane wave (FP-LAPW) method WIEN2k[27] to compute the EUV optical spectra. We employed the linear-response approach of ref 28 which includes the exchange splitting of the core levels, with a Lorentzian broadening of 1.2 eV, and applied a 2.5 eV energy shift of the spectrum to account for the effect of the core hole. The calculated equilibrium spin moments of $Co_{0.50}Pt_{0.50}$ are 1.91 and 0.40 μ_B on Co and Pt, respectively. Although the magnetic moment on Pt is an induced moment, it is sizable enough to provide a clear magnetic signature in the TMOKE measurement. Furthermore, to investigate the approximative influence of magnon excitations on the element-specific demagnetizations, we used the tight-binding linear muffin tin orbitals (TB-LMTO) method[29] together with the disordered local moment method.[30] In these calculations, the influence of a short-wavelength magnon excitation is modeled by a noncollinear arrangement of the Co moments, with an average tilting angle of the moments with respect to the z-axis.[31] Relativistic effects were included by applying the Dirac equation to all electrons. The influence of the (frozen) configuration of Co moments on the Pt moments is self-consistently calculated to access how the Pt moments react to incoherent transverse spin excitations on the Co sublattice.

RESULTS AND DISCUSSION

We start with the static magneto-optical response of Co−Pt alloys in the range 40−72 eV. The magnetic asymmetry measured in TMOKE geometry reveals the characteristic features of Co 3p−3d absorption near 60 eV and two spin−orbit split Pt 5p−5d transitions around 52 and 65 eV (Figure 1a,b) similar to that observed in previous studies.[23,32−34] In contrast to all-optical studies in the near-IR regime, which rely on measuring the response governed by the valence electrons with strongly overlapping wave functions, the EUV probe excites the electrons from the deeper, more localized orbitals. Thus, using dipole selection rules and measuring the magneto-optical response in resonant conditions with one of the atomic transitions, we extract the information about the local magnetic properties in the vicinity of Co or Pt atoms. Figure 1c shows the computed absorptive spectrum of $Co_{0.5}Pt_{0.5}$ in the EUV range, with the main absorption edges denoted in the panel.

To estimate the crosstalk between different spectral components, we performed DFT calculations in which the atomic transitions of the one or another atom were selectively excluded: when all transitions on Pt sites are masked, a strong spectral signature of the Co $M_{2,3}$ transition can be clearly seen near 60.5 eV (Figure 1c, blue trace). It quickly vanishes on the low-energy side, and its contribution to the spectrum at 53 eV is of the order of only 7%, where the Pt O_3 transition dominates. Spectral features of Pt are covering the whole measured spectral range (Figure 1c, red trace), and at 61 eV they are estimated to be ~25% of the total weight, thus partially obscuring the Co response. However, this contrast is high enough for a qualitative study. Throughout the paper, we denote the data for 53 and 61 eV harmonic as Pt and Co responses, respectively.

Short-Time Dynamics and the Demagnetization. Figure 1d shows the time evolution of magnetic asymmetry measured at the Co and Pt resonances for three different pump

https://doi.org/10.1021/acs.jpcc.1c02311
J. Phys. Chem. C 2021, 125, 11714−11721

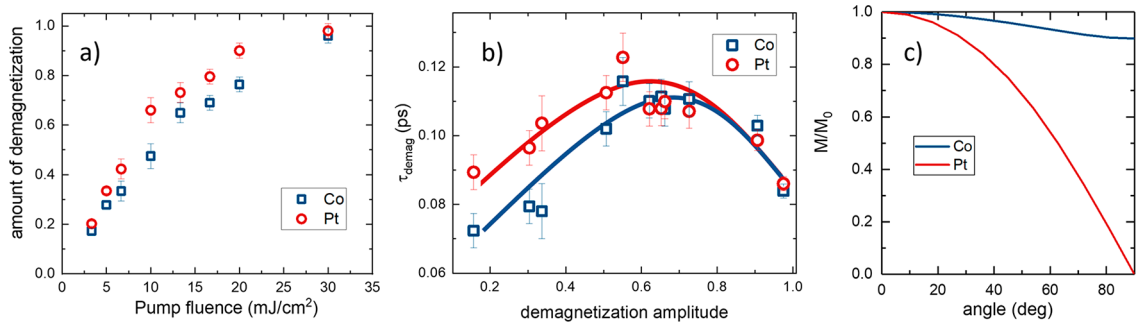

Figure 2. Amounts of demagnetization measured at Co and Pt resonances as a function of the pump fluence, revealing stronger demagnetization of Pt (a). Demagnetization rates measured at Co and Pt resonances for different excitation fluence and 1.5 eV pump photon energy (b). Solid lines are guides for the eye; ab initio calculated change of local magnetizations of Co and of Pt caused by the excitation of transverse spin modes (c). The normalized Co and Pt moments are given as a function of the tilting angle with respect to the *z*-axis.

fluences. The strong excitation of the electronic system by the optical pump is followed by ultrafast demagnetization of the material on an ∼100 fs time scale.[21,23,35] Qualitatively, the response is similar to that detected with all-optical MOKE, which was explained previously by using the microscopic three-temperature model.[21,36] The amount of demagnetization scales with the excitation fluence and is observed at both resonances of Co and Pt. Interestingly, at moderate excitation, the amount of demagnetization at Pt and Co absorption edges is different by 15−25% with Pt revealing a stronger effect for the given pump fluence. The demagnetization for each spectral component as a function of the pump fluence is summarized in Figure 2a. The difference vanishes only at very strong excitations when 100% demagnetization is reached for both sublattices.

In Figure 2b, we summarize the characteristic demagnetization times of Pt and Co responses for different excitation strengths. Here the time constants are measured by fitting an exponential decay function to the demagnetization part of the time traces.

While the film thickness exceeds the penetration depth of the optical pump photons, it is important to note that the observed differences in the dynamics of the two sublattices cannot be explained by the inhomogeneous depth profile of the optical excitation. Because of stronger absorption, it is expected that a thinner layer of the sample is probed near the Co transition compared to Pt absorption edge. However, in this case one would expect to observe stronger demagnetization at Co, which is opposite to what is seen in the experiment.

A closer analysis of the time-delay traces reveals also different demagnetization rates, with Co being slightly faster than Pt (Figure 2b). While qualitatively the dependence of the demagnetization rate on excitation strength resembles the one observed by all-optical MOKE,[21] the present experiments reveal an additional quantitative difference between the two sublattices, which was missed before. For moderate pump fluences the Co demagnetizes with the time constant of 70−110 fs depending on the excitation strength, while Pt demagnetizes on the time scale of 90−120 fs.

Our measurements thus unambiguously detect a stronger demagnetization of Pt as compared to Co as well as a faster demagnetization of Co. To understand the origin of this distinct element-specific demagnetization behavior, it is instructive to compare with other magneto-X-ray measurements on related samples.[19,20,23,34] By investigation of $L1_0$ FePt samples using a combination of XMCD spectroscopy at the Pt L edge and optical polar MOKE spectroscopy, an analogous demagnetization behavior was observed by Yamamoto et al.[19] Conversely, an EUV TMOKE investigation of FePt gave an identical demagnetization of both Fe and Pt.[20] The former experiment[19] had to resort to two separate time-resolved measurements, whereas in the latter experiment[20] the complete data are extracted in a single measurement. However, the proximity of the Fe (52 eV) and Pt edges (53 and 65 eV) can render a separation of their responses problematic, which might explain why an indistinguishable demagnetization was measured.

An investigation of a Co/Pt multilayer using EUV polar MOKE at the Co $M_{2,3}$ edge (60 eV) and Pt $N_{6,7}$ edge (72 eV) showed a faster demagnetization of Co than of Pt and also a stronger demagnetization of Pt,[34] consistent with our measurements. The faster demagnetization of the Co moment was explained by the effect of superdiffusive spin transport[37,38] occurring in the sample at a subpicosecond time scale. The pump laser excitation creates hot spin-polarized electrons in the Co and Pt layers; because of the high initial velocities of the excited electrons (few nanometers per femtosecond), spin-majority electrons leave quickly the Co layer into the surrounding Pt layers, causing thus a fast spin transfer leading to a fast demagnetization of the Co moments (∼80 fs) and, correspondingly, a retarded decay of the Pt moments (∼600 fs). In the Co/Pt multilayer sample the effect of superdiffusion is presumably maximal, but its influence is expected to be less in our Co−Pt alloy sample (see further below), which is consistent with our shorter Pt decay time (90−120 fs). Lastly, a $Co_{0.5}Pt_{0.5}$ alloy sample was investigated with EUV XMCD by Willems et al.[23] at the Co M edge and Pt O_3 and N_7 edges, who found an identical demagnetization of Co and Pt. The identical demagnetization times (∼85 fs) were attributed to optical intersite spin transfer (OISTR),[23,39,40] a process in which the pump laser dominantly excites spin-minority electrons from Pt to Co atoms. It is remarkable that our EUV measurements observe a different behavior, that is, a slower demagnetization on Pt as compared to Co. OISTR takes place during the pump laser pulse,[23] but it cannot be resolved in the present measurements due to limited experimental time resolution. Taking however into account that OISTR would cause an at least equally fast demagnetization of Pt than Co[23] as well as the relatively long time constant of the demagnetization process (<120 fs) compared to the pump pulse length (<35 fs), it is evident that to explain

https://doi.org/10.1021/acs.jpcc.1c02311
J. Phys. Chem. C 2021, 125, 11714−11721

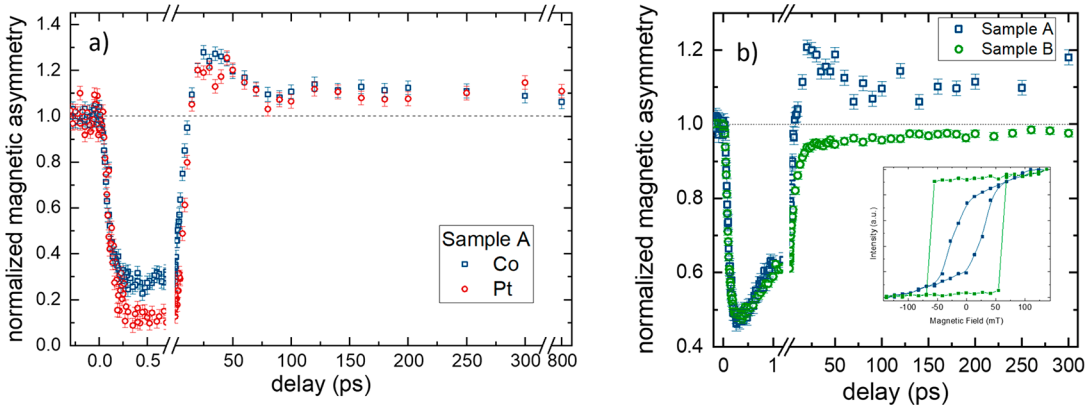

Figure 3. Long time-delay remagnetization traces measured at the Co and Pt absorption edges for sample A (a). Comparison of remagnetization curves for two samples measured at the Co absorption edge (b). The pump fluence was adjusted to have similar amounts of demagnetization in the two samples. The inset shows the respective in-plane hysteresis loops.

our measurements additional processes must be considered. OISTR is also predicted[23] to lead to a larger demagnetization of Co than of Pt at 80 fs, which is not visible in our measurements.

In the initial stage of demagnetization, immediately after the pump pulse, hot spin-polarized electrons excited on the Co and Pt atoms have large velocities and will move fast through the sample. These hot electrons thermalize and lose mobility while they scatter with other electrons and immobilize at both Co and Pt atoms. This electron thermalization process is completed in about 150−200 fs. As Co spin-majority hot electrons have higher velocities than spin-minority electrons,[37] they will redistribute more within the sample and cause a faster loss of spin moment on the Co atoms and a slower demagnetization on Pt. In these first few hundred femtoseconds, energy is being transferred from the hot electrons to other electrons and to phonons and magnons exciting hot incoherent phonons and magnons.[1,36]

We propose that the stronger demagnetization measured at Pt sites can be related to the induced nature of Pt moments and their strong sensitivity to the orientation of the "driving" Co moments. When incoherent transverse magnons are excited through the nonequilibrium hot electrons, the average angle between the Co moments is altered. In an adiabatic picture the canting of the Co moments weakens the exchange interactions on the Pt atoms, thereby effectively weakening also the magnetic moment at the Pt sites. Our DFT calculations confirm that the thus-caused difference in the amount of demagnetization between the two sublattices is substantial already for quite small average angles of the Co moments (Figure 2c). The calculations show that the Co moments display a Heisenberg-type behavior; that is, the magnitude of the atomic spin moment hardly changes when the average angle of the moments with respect to the *z*-axis is changed. For the Pt moment, however, its induced nature is pivotal for the much stronger reduction of the moment. A similar effect was previously observed for $L1_0$ FePt samples[19] but by using two different magnetic spectroscopies. The advantage of our experiment is that the complete data are extracted from a single measurement.

We note that the observed difference in the dynamics of the two components is not unique to the sample presented here (sample A) but also can be observed in the samples with different magnetic anisotropy (sample B) or with different Pt content (tested in the range 30−50%).

Remagnetization Dynamics. After ∼0.5 ps the sample starts to recover toward the equilibrium magnetization state. Naturally, the effect is extremely sensitive to the details of heat dissipation in the system, sample structure, and excitation strength. The long-time traces measured at Co and Pt absorption edges are shown in Figure 3a for sample A grown on Si/SiOx. The behavior of the system is similar at both resonances. The time constant of the recovery process increases with the pump fluence. Interestingly, the magnetic asymmetry does not recover to the static value ($M/M_0 = 1$) but a larger value $M/M_0 \sim 1.2$. On top of the exponential recovery, we observe a periodic signal with a period of 100 ± 15 ps. The value of the normalized magnetic asymmetry at long delays (i.e., the magnitude of the overshoot) increases with increasing the pump fluence.

We attribute the overshoot in magnetic asymmetry to the heat-induced change of magnetic anisotropy of the sample: despite having mainly in-plane easy magnetization direction, the sample has a finite out-of-plane component of the magnetization, which can be confirmed by the slope of the hysteresis loop at high magnetic fields (Figure 3b, inset: sample A). Laser heating of the system causes magnetic moments to reorient and start precessing around the new equilibrium. Because in the TMOKE geometry only the in-plane projection of the magnetic moment is detected, the reorientation of the magnetization toward the sample plane will be observed as an enhancement of the magnetic asymmetry. The oscillating part of the signal is caused by the coherent precessional motion around the new quasi-equilibrium. The observed period of oscillations matches well the FMR mode of Co−Pt.

The magnetic asymmetry stays at the enhanced level for at least 800 ps, which is the maximum delay our experimental setup can provide. Because the effect is purely driven by the heating of the lattice, the recovery can take up to microseconds, depending on the thermal contact between the sample and the external bath.

To prove our hypothesis, we performed similar experiments on the sample with the same stoichiometry but *c*-axis aligned in the plane of the sample (sample B). To achieve better alignment of the spins, the Co−Pt film was grown on top of an epitaxial layer of Cr on MgO(110).[41] The corresponding

https://doi.org/10.1021/acs.jpcc.1c02311
J. Phys. Chem. C 2021, 125, 11714−11721

hysteresis loop is plotted in Figure 3b (inset). Both hysteresis loops are normalized to the magnetization at 200 mT.

Figure 3b shows the time dynamics of the magnetic asymmetry for both samples measured at Co absorption edge and external field of ±200 mT. The pump pulse power was adjusted to achieve comparable amounts of demagnetization in both samples. In sample B we observe monotonous recovery of the magnetic state toward the equilibrium value with no overshoot. Because the only parameter that was varied is the alignment of the magnetic moments, while the sample stoichiometry stayed constant, we confirm that the heat-induced change of the magnetic anisotropy is a plausible explanation for the apparent overshoot in sample A. A small difference in the remagnetization times for the two samples is presumably related to better heat dissipation in sample A.

These observations highlight the importance of studying the complete magnetization state of the sample and not just a single projection of the total magnetic moment.

CONCLUSIONS

In conclusion, we have studied the ultrafast spin dynamics of Co−Pt alloys employing element-specific resonant TMOKE spectroscopy in the EUV range. We observed that the induced nature of magnetic moments of Pt does not necessarily imply that their dynamics are equal to the dynamics of the driving Co moments. Specifically, in Co−Pt alloy we observe that the demagnetization rate and the amplitude of the demagnetization are larger at Pt sites as compared to Co. The differences in the amount of demagnetization can be explained by the modification of the exchange interaction at the Pt site when incoherent transverse spin modes are excited. The observed slower demagnetization on the Pt sublattice is unlikely due to optical intersite spin transfer as this would cause a faster demagnetization on Pt during the pump pulse. The different time scales of the two sublattices' demagnetizations are presumably caused by a redistribution of hot spin-polarized electrons in the sample after the pump pulse. Lastly, we also showed that the time evolution of the magnetic anisotropy after the laser excitation has to be carefully analyzed to avoid any experimental artifacts caused by measuring a single projection of the total magnetic moment, as is done in the vast majority of ultrafast magnetism experiments.

AUTHOR INFORMATION

Corresponding Authors

Igor Vaskivskyi − *Center for Memory and Recording Research, University of California, San Diego, La Jolla, California 92093-0401, United States; Department of Physics and Astronomy, Uppsala University, 75120 Uppsala, Sweden*; Email: igor.vaskivskyi@ijs.si

Hermann A. Dürr − *Department of Physics and Astronomy, Uppsala University, 75120 Uppsala, Sweden*; orcid.org/0000-0001-9680-8730; Email: hermann.durr@physics.uu.se

Authors

Rameez Saeed Malik − *Department of Physics and Astronomy, Uppsala University, 75120 Uppsala, Sweden*

Leandro Salemi − *Department of Physics and Astronomy, Uppsala University, 75120 Uppsala, Sweden*

Diego Turenne − *Department of Physics and Astronomy, Uppsala University, 75120 Uppsala, Sweden*

Ronny Knut − *Department of Physics and Astronomy, Uppsala University, 75120 Uppsala, Sweden*

Jeffrey Brock − *Center for Memory and Recording Research, University of California, San Diego, La Jolla, California 92093-0401, United States*

Robert Stefanuik − *Department of Physics and Astronomy, Uppsala University, 75120 Uppsala, Sweden*

Johan Söderström − *Department of Physics and Astronomy, Uppsala University, 75120 Uppsala, Sweden*

Karel Carva − *Faculty of Mathematics and Physics, Department of Condensed Matter Physics, Charles University, 121 16 Prague, Czech Republic*

Eric E. Fullerton − *Center for Memory and Recording Research, University of California, San Diego, La Jolla, California 92093-0401, United States*

Peter M. Oppeneer − *Department of Physics and Astronomy, Uppsala University, 75120 Uppsala, Sweden*

Olof Karis − *Department of Physics and Astronomy, Uppsala University, 75120 Uppsala, Sweden*; orcid.org/0000-0001-6406-217X

Complete contact information is available at: https://pubs.acs.org/10.1021/acs.jpcc.1c02311

Notes

The authors declare no competing financial interest.

ACKNOWLEDGMENTS

I.V., J.B., and E.E.F. acknowledge support by the U.S. Department of Energy, Office of Science, Office of Basic Energy Sciences under the X-ray Scattering Program Award DE-SC0017643. D.T., P.M.O., and H.A.D. acknowledge support from the Swedish Research Council (VR). P.M.O. acknowledges support from the K. and A. Wallenberg Foundation (Grant 2015.0060). The calculations were enabled by resources provided by the Swedish National Infrastructure for Computing (SNIC) at NSC Linköping, partially funded by VR through Grant Agreement 2018-05973.

REFERENCES

(1) Beaurepaire, E.; Merle, J.-C.; Daunois, A.; Bigot, J.-Y. Ultrafast Spin Dynamics in Ferromagnetic Nickel. *Phys. Rev. Lett.* **1996**, *76*, 4250−4253.

(2) Koopmans, B.; van Kampen, M.; Kohlhepp, J. T.; de Jonge, W. J. M. Ultrafast Magneto-Optics in Nickel: Magnetism or Optics? *Phys. Rev. Lett.* **2000**, *85*, 844−847.

(3) Kirilyuk, A.; Kimel, A. V.; Rasing, T. Ultrafast Optical Manipulation of Magnetic Order. *Rev. Mod. Phys.* **2010**, *82*, 2731−2784.

(4) Stanciu, C. D.; Tsukamoto, A.; Kimel, A. V.; Hansteen, F.; Kirilyuk, A.; Itoh, A.; Rasing, Th Subpicosecond Magnetization Reversal across Ferrimagnetic Compensation Points. *Phys. Rev. Lett.* **2007**, *99*, 217204.

(5) Ostler, T. A.; Barker, J.; Evans, R. F. L.; Chantrell, R. W.; Atxitia, U.; Chubykalo-Fesenko, O.; El Moussaoui, S.; Le Guyader, L.; Mengotti, E.; Heyderman, L. J.; et al. Ultrafast Heating as a Sufficient Stimulus for Magnetization Reversal in a Ferrimagnet. *Nat. Commun.* **2012**, *3*, 666.

(6) Alebrand, S.; Gottwald, M.; Hehn, M.; Steil, D.; Cinchetti, M.; Lacour, D.; Fullerton, E. E.; Aeschlimann, M.; Mangin, S. Light-Induced Magnetization Reversal of High-Anisotropy TbCo Alloy Films. *Appl. Phys. Lett.* **2012**, *101*, 162408.

(7) Radu, I.; Vahaplar, K.; Stamm, C.; Kachel, T.; Pontius, N.; Dürr, H. A.; Ostler, T. A.; Barker, J.; Evans, R. F. L.; Chantrell, R. W.; et al. Transient Ferromagnetic-like State Mediating Ultrafast Reversal of Antiferromagnetically Coupled Spins. *Nature* **2011**, *472*, 205−208.

(8) Graves, C. E.; Reid, A. H.; Wang, T.; Wu, B.; de Jong, S.; Vahaplar, K.; Radu, I.; Bernstein, D. P.; Messerschmidt, M.; Müller, L.; et al. Nanoscale Spin Reversal by Non-Local Angular Momentum Transfer Following Ultrafast Laser Excitation in Ferrimagnetic GdFeCo. *Nat. Mater.* **2013**, *12*, 293−298.
(9) Liu, T.-M.; Wang, T.; Reid, A. H.; Savoini, M.; Wu, X.; Koene, B.; Granitzka, P.; Graves, C. E.; Higley, D. J.; Chen, Z.; et al. Nanoscale Confinement of All-Optical Magnetic Switching in TbFeCo - Competition with Nanoscale Heterogeneity. *Nano Lett.* **2015**, *15*, 6862−6868.
(10) Mangin, S.; Gottwald, M.; Lambert, C.-H.; Steil, D.; Uhlíř, V.; Pang, L.; Hehn, M.; Alebrand, S.; Cinchetti, M.; Malinowski, G.; et al. Engineered Materials for All-Optical Helicity-Dependent Magnetic Switching. *Nat. Mater.* **2014**, *13*, 286−292.
(11) Lambert, C.-H.; Mangin, S.; Varaprasad, B. S. D. C. S.; Takahashi, Y. K.; Hehn, M.; Cinchetti, M.; Malinowski, G.; Hono, K.; Fainman, Y.; Aeschlimann, M.; et al. All-Optical Control of Ferromagnetic Thin Films and Nanostructures. *Science* **2014**, *345*, 1337−1340.
(12) Ellis, M. O. A.; Fullerton, E. E.; Chantrell, R. W. All-Optical Switching in Granular Ferromagnets Caused by Magnetic Circular Dichroism. *Sci. Rep.* **2016**, *6*, 30522.
(13) Kichin, G.; Hehn, M.; Gorchon, J.; Malinowski, G.; Hohlfeld, J.; Mangin, S. From Multiple- to Single-Pulse All-Optical Helicity-Dependent Switching in Ferromagnetic Co/Pt Multilayers. *Phys. Rev. Appl.* **2019**, *12*, 024019.
(14) Yamada, K. T.; Kimel, A. V.; Ruta, S.; Chantrell, R.; Prabhakara, K. H.; Li, T.; Ando, F.; Semin, S.; Ono, T.; Kirilyuk, A.; et al. All-Optical Switching of Spins in Ferromagnetic Co/Pt with a Single Dual Pulse. *arXiv:1903.01941* **2020**.
(15) Vomir, M.; Albrecht, M.; Bigot, J.-Y. Single Shot All Optical Switching of Intrinsic Micron Size Magnetic Domains of a Pt/Co/Pt Ferromagnetic Stack. *Appl. Phys. Lett.* **2017**, *111*, 242404.
(16) Gorchon, J.; Lambert, C.-H.; Yang, Y.; Pattabi, A.; Wilson, R. B.; Salahuddin, S.; Bokor, J. Single Shot Ultrafast All Optical Magnetization Switching of Ferromagnetic Co/Pt Multilayers. *Appl. Phys. Lett.* **2017**, *111*, 042401.
(17) Igarashi, J.; Remy, Q.; Iihama, S.; Malinowski, G.; Hehn, M.; Gorchon, J.; Hohlfeld, J.; Fukami, S.; Ohno, H.; Mangin, S. Engineering Single-Shot All-Optical Switching of Ferromagnetic Materials. *Nano Lett.* **2020**, *20*, 8654−8660.
(18) Cornelissen, T. D.; Córdoba, R.; Koopmans, B. Microscopic Model for All Optical Switching in Ferromagnets. *Appl. Phys. Lett.* **2016**, *108*, 142405.
(19) Yamamoto, K.; Kubota, Y.; Suzuki, M.; Hirata, Y.; Carva, K.; Berritta, M.; Takubo, K.; Uemura, Y.; Fukaya, R.; Tanaka, K.; et al. Ultrafast Demagnetization of Pt Magnetic Moment in L10-FePt Probed by Magnetic Circular Dichroism at a Hard x-Ray Free Electron Laser. *New J. Phys.* **2019**, *21*, 123010.
(20) Hofherr, M.; Moretti, S.; Shim, J.; Häuser, S.; Safonova, N. Y.; Stiehl, M.; Ali, A.; Sakshath, S.; Kim, J. W.; Kim, D. H.; et al. Induced versus Intrinsic Magnetic Moments in Ultrafast Magnetization Dynamics. *Phys. Rev. B: Condens. Matter Mater. Phys.* **2018**, *98*, 174419.
(21) Kuiper, K. C.; Roth, T.; Schellekens, A. J.; Schmitt, O.; Koopmans, B.; Cinchetti, M.; Aeschlimann, M. Spin-Orbit Enhanced Demagnetization Rate in Co/Pt-Multilayers. *Appl. Phys. Lett.* **2014**, *105*, 202402.
(22) Hecker, M.; Oppeneer, P. M.; Valencia, S.; Mertins, H.-Ch.; Schneider, C. M. Soft X-Ray Magnetic Reflection Spectroscopy at the 3p Absorption Edges of Thin Fe Films. *J. Electron Spectrosc. Relat. Phenom.* **2005**, *144−147*, 881−884.
(23) Willems, F.; von Korff Schmising, C.; Strüber, C.; Schick, D.; Engel, D. W.; Dewhurst, J. K.; Elliott, P.; Sharma, S.; Eisebitt, S. Optical Inter-Site Spin Transfer Probed by Energy and Spin-Resolved Transient Absorption Spectroscopy. *Nat. Commun.* **2020**, *11*, 871.
(24) Plogmaker, S.; Terschlüsen, J. A.; Krebs, N.; Svanqvist, M.; Forsberg, J.; Cappel, U. B.; Rubensson, J.-E.; Siegbahn, H.; Söderström, J. HELIOS—A Laboratory Based on High-Order Harmonic Generation of Extreme Ultraviolet Photons for Time-Resolved Spectroscopy. *Rev. Sci. Instrum.* **2015**, *86*, 123107.
(25) Stefanuik, R.; Knut, R.; Jana, S.; Terschlüsen, J. A.; Sandell, A.; Söderström, J. Developments and Enhancements to the HELIOS Pump Probe System. *J. Electron Spectrosc. Relat. Phenom.* **2018**, *224*, 33−37.
(26) Jana, S.; Terschlüsen, J. A.; Stefanuik, R.; Plogmaker, S.; Troisi, S.; Malik, R. S.; Svanqvist, M.; Knut, R.; Söderström, J.; Karis, O. A Setup for Element Specific Magnetization Dynamics Using the Transverse Magneto-Optic Kerr Effect in the Energy Range of 30−72 EV. *Rev. Sci. Instrum.* **2017**, *88*, 033113.
(27) Blaha, P.; Schwarz, K.; Madsen, G.; Kvasnicka, D.; Luitz, J. *WIEN2k: An Augmented Plane Wave plus Local Orbitals Program for Calculating Crystal Properties*; Technische Universität Wien: Vienna, Austria, 2001.
(28) Valencia, S.; Kleibert, A.; Gaupp, A.; Rusz, J.; Legut, D.; Bansmann, J.; Gudat, W.; Oppeneer, P. M. Quadratic X-Ray Magneto-Optical Effect upon Reflection in a Near-Normal-Incidence Configuration at the M Edges of 3d-Transition Metals. *Phys. Rev. Lett.* **2010**, *104*, 187401.
(29) Turek, I.; Drchal, V.; Kudrnovsky, J.; Sob, M.; Weinberger, P. *Electronic Structure of Disordered Alloys, Surfaces and Interfaces*; Springer: Boston, MA, 1997.
(30) Staunton, J.; Gyorffy, B. L.; Pindor, A. J.; Stocks, G. M.; Winter, H. Electronic Structure of Metallic Ferromagnets above the Curie Temperature. *J. Phys. F: Met. Phys.* **1985**, *15*, 1387.
(31) Wagenknecht, D.; Šmejkal, L.; Kašpar, Z.; Sinova, J.; Jungwirth, T.; Kudrnovský, J.; Carva, K.; Turek, I. Temperature-Dependent Resistivity and Anomalous Hall Effect in NiMnSb from First Principles. *Phys. Rev. B: Condens. Matter Mater. Phys.* **2019**, *99*, 174433.
(32) Shishidou, T.; Imada, S.; Muro, T.; Oda, F.; Kimura, A.; Suga, S.; Miyahara, T.; Kanomata, T.; Kaneko, T. Strong Fano Effect in the Magnetic Circular Dichroism of the Pt N6,7 Core Absorption of Ferromagnetic CoPt3. *Phys. Rev. B: Condens. Matter Mater. Phys.* **1997**, *55*, 3749−3756.
(33) Willems, F.; Smeenk, C. T. L.; Zhavoronkov, N.; Kornilov, O.; Radu, I.; Schmidbauer, M.; Hanke, M.; von Korff Schmising, C.; Vrakking, M. J. J.; Eisebitt, S. Probing Ultrafast Spin Dynamics with High-Harmonic Magnetic Circular Dichroism Spectroscopy. *Phys. Rev. B: Condens. Matter Mater. Phys.* **2015**, *92*, 220405.
(34) Yamamoto, K.; Moussaoui, S. E.; Hirata, Y.; Yamamoto, S.; Kubota, Y.; Owada, S.; Yabashi, M.; Seki, T.; Takanashi, K.; Matsuda, I.; et al. Element-Selectively Tracking Ultrafast Demagnetization Process in Co/Pt Multilayer Thin Films by the Resonant Magneto-Optical Kerr Effect. *Appl. Phys. Lett.* **2020**, *116*, 172406.
(35) Moisan, N.; Malinowski, G.; Mauchain, J.; Hehn, M.; Vodungbo, B.; Lüning, J.; Mangin, S.; Fullerton, E. E.; Thiaville, A. Investigating the Role of Superdiffusive Currents in Laser Induced Demagnetization of Ferromagnets with Nanoscale Magnetic Domains. *Sci. Rep.* **2015**, *4*, 4658.
(36) Koopmans, B.; Malinowski, G.; Dalla Longa, F.; Steiauf, D.; Fähnle, M.; Roth, T.; Cinchetti, M.; Aeschlimann, M. Explaining the Paradoxical Diversity of Ultrafast Laser-Induced Demagnetization. *Nat. Mater.* **2010**, *9*, 259−265.
(37) Battiato, M.; Carva, K.; Oppeneer, P. M. Theory of Laser-Induced Ultrafast Superdiffusive Spin Transport in Layered Heterostructures. *Phys. Rev. B: Condens. Matter Mater. Phys.* **2012**, *86*, 024404.
(38) Battiato, M.; Carva, K.; Oppeneer, P. M. Superdiffusive Spin Transport as a Mechanism of Ultrafast Demagnetization. *Phys. Rev. Lett.* **2010**, *105*, 027203.
(39) Dewhurst, J. K.; Elliott, P.; Shallcross, S.; Gross, E. K. U.; Sharma, S. Laser-Induced Intersite Spin Transfer. *Nano Lett.* **2018**, *18*, 1842−1848.
(40) Siegrist, F.; Gessner, J. A.; Ossiander, M.; Denker, C.; Chang, Y.-P.; Schröder, M. C.; Guggenmos, A.; Cui, Y.; Walowski, J.; Martens, U.; et al. Light-Wave Dynamic Control of Magnetism. *Nature* **2019**, *571*, 240−244.

https://doi.org/10.1021/acs.jpcc.1c02311
J. Phys. Chem. C 2021, 125, 11714−11721

(41) Yao, Y. D.; Liou, Y.; Huang, J. C. A.; Liao, S. Y.; Klik, I.; Yang, W. T.; Chang, C. P.; Lo, C. K. Enhancement of Magnetoresistance in Co(1100)/Cr(211) Bilayered Films on MgO(110). *J. Appl. Phys.* **1996**, *79*, 6533−6535.

https://doi.org/10.1021/acs.jpcc.1c02311
J. Phys. Chem. C 2021, 125, 11714−11721